ized, then the predicted "critical" ester concentration (at which discrete collapse first occurs) would be given by f_c/n, or 0.57%, 0.30%, and 0.18% for n = 200, 500, and 1000, respectively. Since the observed critical ester concentration lies between 1.6 and 2%, these predicted values are all clearly too small.

We have assumed that all of the doped ester units, after polymerization, are fully ionized. However, it is known that in a polymer solution of poly(acrylic acid), only about 20% of the ionizable units are effectively ionized. Hence, if we were to assume a similar fraction of ionization for our ester units, the effective experimental critical ester concentration would lie between 0.32 and 0.40%. In this case, the predicted range of theoretical values for f_c/n agrees with our findings. These calculations, of course, are meant only to provide qualitative verification of the experimental results. A more careful analysis would be required to obtain quantitative agreement. (For example, Ilavsky[5] has shown that the free energy of electrostatic repulsions influences the swelling of ionic gels; this contribution should therefore be included in eq 1. Because this repulsive interaction increases the stiffness of the gel, the value of f is effectively increased.)

In conclusion, we have prepared acrylamide gels that can be ionized to differing degrees by changing the amount of an ionizable ester that is incorporated into the polyacrylamide network. In so doing, we have directly confirmed in a qualitative way the hypothesis that the behavior of the gel swelling ratio with respect to solvent composition depends on the degree of ionization of the gel network. Future related experiments based on chemical modifications of gels should prove useful in exploring the details of the phase transitions observed in ionic gels.

Acknowledgment. We thank Izumi Nishio and Shao-Tang Sun for helpful comments. D.N. thanks T.T. for his hospitality during the former's sabbatical-leave visit at MIT, where the experimental work was performed. This work was supported in part by the Office of Naval Research, Grant No. N00014-80-C-0050.

References and Notes

(1) Tanaka, T. *Phys. Rev. Lett.* **1978**, *40*, 820.
(2) Tanaka, T.; Fillmore, D.; Sun, S. T.; Nishio, I.; Swislow, G.; Shah, A. *Phys. Rev. Lett.* **1980**, *45*, 1636.
(3) Flory, P. J. "Principles of Polymer Chemistry"; Cornell University Press: Ithaca, NY, 1953.
(4) The possibility of a discrete transition in a nonionized gel has been predicted by: Dusek, K.; Patterson, D. *J. Polym. Sci., Part A-2* **1968**, *6*, 1209.
(5) Ilavsky, M. *Polymer* **1981**, *22*, 1687.
(6) Pollak, A.; Blumenfeld, H.; Wax, M.; Baughn, R. L.; Whitesides, G. M. *J. Am. Chem. Soc.* **1980**, *102*, 6324.
(7) Sandler, S. R.; Karo, W. "Polymer Synthesis"; Academic Press: New York, 1977; Vol. II, pp 271–305.
(8) Janus, V. F.; Rodriguez, F.; Cohen, C. *Macromolecules* **1980**, *13*, 977.

Pressure Dependence of the Glass Transition in *cis*-Polyisoprene As Studied by Dielectric Relaxation

Eddy N. Dalal and Paul J. Phillips*

Department of Materials Science and Engineering, University of Utah, Salt Lake City, Utah 84112. *Received August 24, 1982*

ABSTRACT: Dielectric relaxation studies of the glass transition in *cis*-polyisoprene have been carried out between atmospheric pressure and 3.8 kbar. A procedure based on the Williams–Landel–Ferry (WLF) free volume formulation has been developed to analyze these data and obtain the glass transition temperature T_g and the WLF parameters $U^* = 2.3Rc_1c_2$ and $T_\infty = T_g - c_2$ as functions of pressure. The variation of T_g with pressure can be well represented by $T_g(P) = -72.0 + 17.78P - 0.673P^2$, and c_2 rises by about 8%/kbar. It is demonstrated that values of dT_g/dP obtained from data at a constant experimental frequency give rise to misleadingly high values of that coefficient. Cole–Cole analyses show that at a given pressure, the distribution of relaxation times decreases with increasing temperature. For a given relaxation time the Cole–Cole parameter, α, increases with pressure.

Introduction

cis-Polyisoprene, generally in the form of natural rubber from *hevea brasiliensis*, is a very important commercial polymer. Its elastic properties have been extensively investigated and are limited, as in all elastomers, by proximity to the glass transition temperature. Although elevated pressures are used in the processing of the polymer and often in service, studies of the effects of pressure on its properties are few. The only report in the literature of the effect of pressure on relaxation behavior is related to the dynamic compressibility of a cross-linked specimen (12% sulfur) at pressures up to 1 kbar.[1] The researchers reported a dT_g/dP coefficient of 24 °C/kbar. They also reported that the WLF equation[2] could be used to superpose data with invariant values of c_1 and c_2 for the frequency range studied (50–1000 Hz).

Recently, pressure–volume data have been reported over an extensive pressure range (to 8 kbar) but a narrow temperature range (15–40 °C), for which a dT_g/dP coefficient of 13 °C/kbar was deduced from the data.[3]

Dielectric relaxation studies of *cis*-polyisoprene at atmospheric pressure have been reported by Norman[4] for the frequency range 50 Hz to 1 MHz. Relaxation processes are observed in natural rubber largely because of the presence of adventitious dipoles resulting from oxidation.

The purpose of the work being reported here was to study the dielectric relaxation behavior of natural rubber at pressures up to 4 kbar, to obtain values of T_g and dT_g/dP as a function of pressure, and to investigate the applicability of the WLF equation over the pressure range studied. It is based on part of a Ph.D. Dissertation,[5] in which the experimentation and processing of dielectric data are described in greater detail.

Experimental Section

Specimen Preparation. The natural rubber used was a grade of pale crepe supplied by the Malaysian Rubber Producers Research Association, Brickendonbury, England. It was Soxhlet extracted with benzene in order to remove the stearic acid and

0024-9297/83/2216-0890$01.50/0

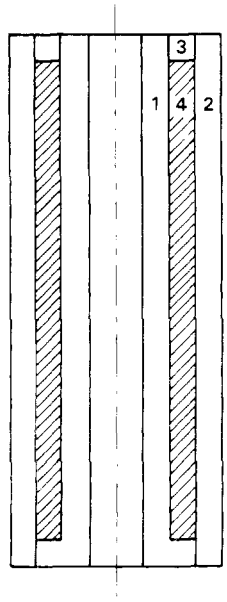

Figure 1. Schematic section of the composite specimen. Hollow polyethylene cylinders (1, 2) and an endcap (3) surround the *cis*-polyisoprene sample (4).

other impurities normally present.

Because of the low temperatures used in these studies, isopentane was used as the pressurizing fluid in the dielectric studies. Unfortunately, isopentane swells *cis*-polyisoprene, making it necessary to encapsulate the rubber specimen in unoxidized high-density polyethylene. Since a coaxial dielectric cell was used, a composite specimen was fabricated having the cross section shown in Figure 1. Hollow cylinders and end caps were first machined out of essentially loss-free high-density polyethylene. Rubber was then placed in the hollow section, pressed into place, and allowed to relax under vacuum at ~60 °C. The final stage was the fusing on of the end caps in a support mold in the hot press. Specimens made in this manner were stable in contact with isopentane and could be reused several times.

High-Pressure Dielectric Equipment. The system used was the one already described by Sayre et al.[6] with a modification that permitted better subambient temperature control and much easier refilling of the pressurizing system. Experimentation was carried out by first applying the required pressure at room temperature and then cooling down to ~30 °C below the glass transition temperature at that pressure, continually adjusting the equipment to maintain the required pressure. The system was then warmed up by alternately turning the heaters on and off for short periods, resulting in a succession of short temperature ramps separated by plateaus. Dielectric measurements were made on a General Radio 1621 capacitance measurement system during the approximately isothermal periods.

Results

Since the raw capacitance and conductance data were obtained for a composite sample, the data were processed[5] in such a way as to extract the dielectric constant and loss of the rubber using known data for high-density polyethylene[6] and isopentane[7] together with the dimensions of the specimen. A subtractive procedure was used to correct for dc conductivity in isopentane; however, some uncertainty remains in the high-temperature end of the low-frequency loss data due to this effect. The dc conductivity was suppressed by pressure, as might be expected for ionic conduction, thus permitting dielectric data to be obtained at the higher temperatures involved.

Data obtained at atmospheric pressure, together with dielectric loss data only obtained at 0.34, 0.69, 1.72, 2.41, 3.45, and 3.79 kbar, are presented in Figures 2–8. The high-pressure dielectric constant data may be found in ref 5 and are not of major importance in this article. At

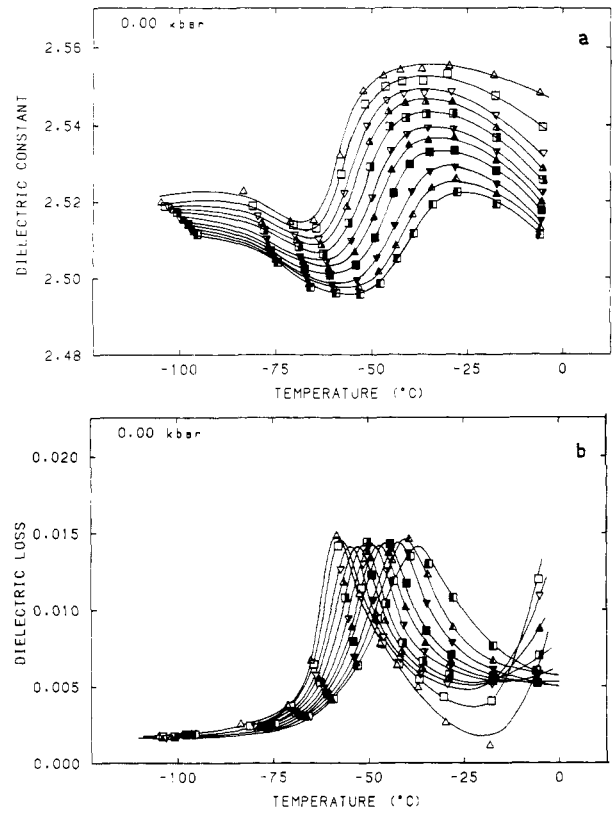

Figure 2. Dielectric constant (a) and loss (b) at atmospheric pressure. Symbols refer to frequencies of 10 Hz (△), 20 Hz (□), 50 Hz (▽), 100 Hz (▲), 200 Hz (▣), 500 Hz (▼), 1 kHz (▲), 2 kHz (■), 5 kHz (▼), 10 kHz (▲) and 20 kHz (◧).

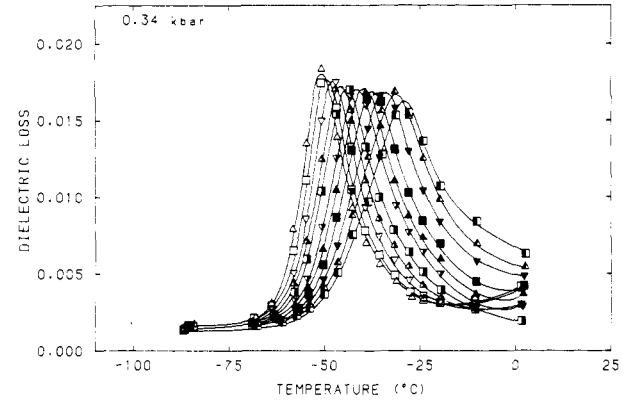

Figure 3. Dielectric loss at 0.34 kbar. Symbols as in Figure 2.

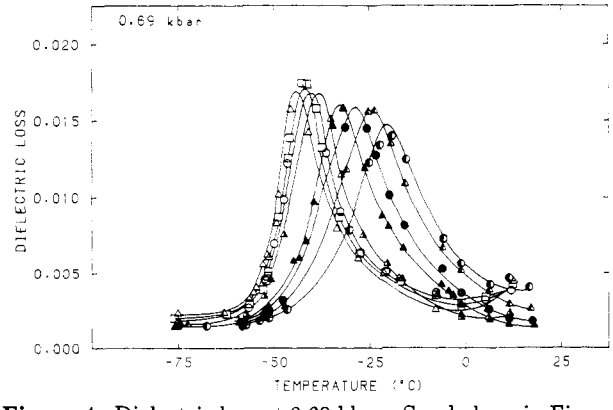

Figure 4. Dielectric loss at 0.69 kbar. Symbols as in Figure 2, plus 30 Hz (○), 3 kHz (●), and 30 kHz (◑).

elevated pressures all the curves shift to higher temperatures, as expected. The dielectric constant falls with in-

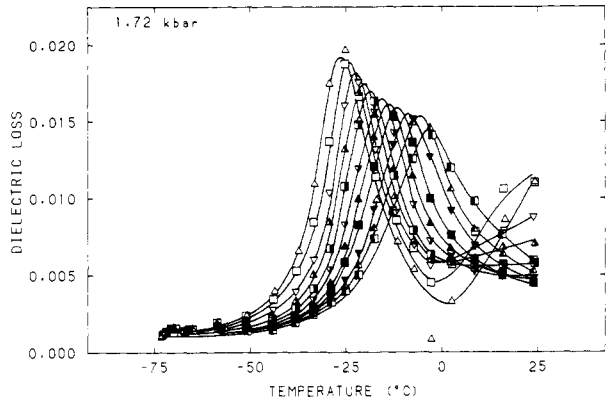

Figure 5. Dielectric loss at 1.72 kbar. Symbols as in Figure 2.

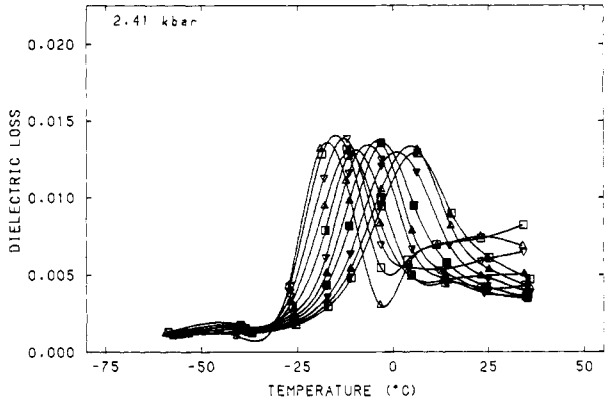

Figure 6. Dielectric loss at 2.41 kbar. Symbols as in Figure 2.

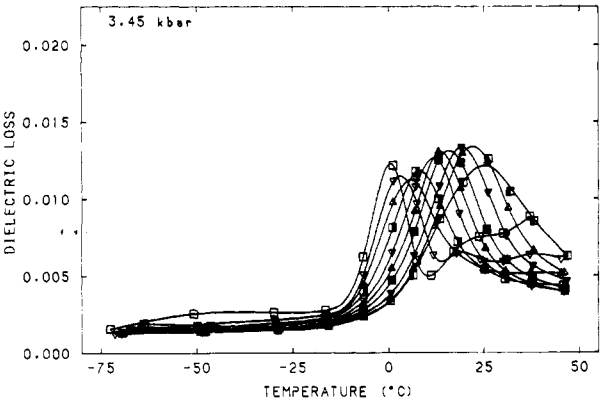

Figure 7. Dielectric loss at 3.45 kbar. Symbols as in Figure 2.

creasing temperature outside the relaxation region; this may be attributed to thermal expansion and is compatible with the Clausius–Mosotti equation. Dielectric loss curves at each pressure show a distinct broadening with increasing temperature. A single relaxation process is present in the experimental temperature range.

The data obtained at atmospheric pressure are in substantial accord with those published by Norman.[4] Whereas the absolute magnitude of both the dielectric constant and loss varies from sample to sample with variations in adventitious dipole concentration and isopentane conductivity, single data curves are produced (Figure 9) when Arrhenius plots are made of dielectric loss peak frequency vs. temperature. Data of Norman[4] and the more recent data of Bakule and Stoll[8] are also presented in Figure 9 for comparison.

Arrhenius plots are presented in Figure 10 for all the pressures studied. The plots are shifted to higher temperatures as pressure is increased. They also show a gradual steepening with pressure; however, since the plots

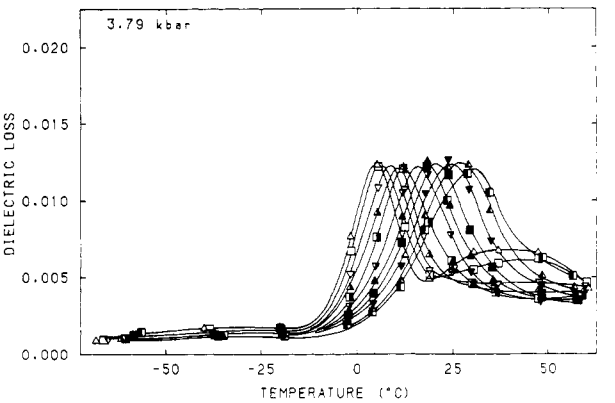

Figure 8. Dielectric loss at 3.79 kbar. Symbols as in Figure 2.

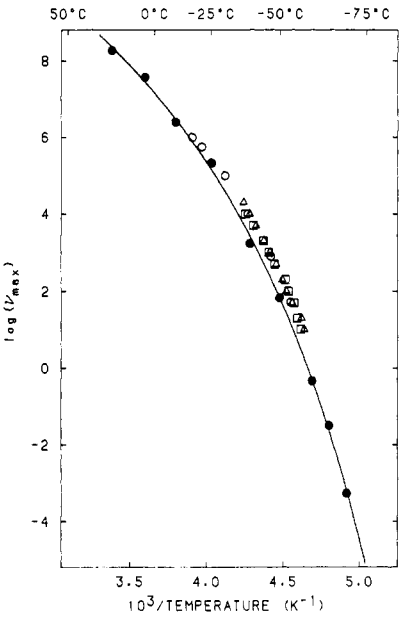

Figure 9. Arrhenius plot of data at atmospheric pressure: (△, □) our data from two different runs using different samples; (○) data of Norman;[4] (●) data of Bakule and Stoll.[7]

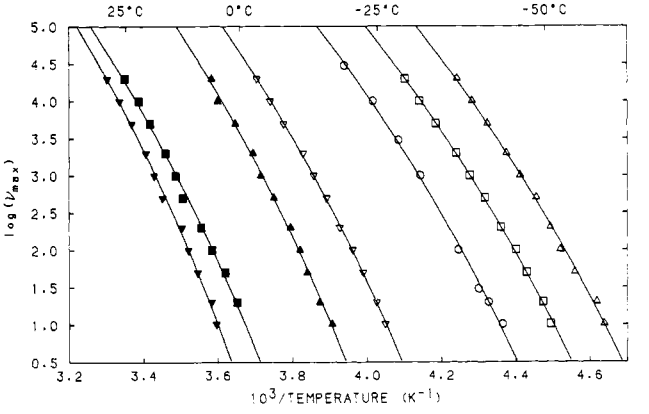

Figure 10. Arrhenius plots of the data obtained at the following pressures: atmospheric (△), 0.34 kbar (□), 0.69 kbar (○), 1.72 kbar (▽), 2.41 kbar (▲), 3.45 kbar (■), and 3.79 kbar (▼).

are all curved, a simple Arrhenius analysis was not carried out. The analysis used will be discussed in detail in the next section.

Discussion

Since there are two important and quite different points to be analyzed, this section will be split into subsections dealing with (a) the extraction of the glass transition and WLF constants from the data and their variation with

pressure and (b) the effect of pressure on the distribution of relaxation times.

Time–Temperature–Pressure Analyses. Despite extensive investigations of the dielectric relaxation behavior under pressure of several polymers[9-11] a method for the extraction of glass transition temperatures from the raw data has never been published. Simply assuming that the actual T_g varies identically with loss peak temperature at a constant experimental frequency seriously overestimates the pressure dependence of T_g, as will be demonstrated later in this section.

Two basic assumptions are necessary in order to process the data. These are (a) that there is a characteristic constant frequency at which the glass transition, as observed in a scanning experiment, occurs independent of pressure and (b) that there is a characteristic constant free volume at which the glass transition occurs. The latter assumption is acknowledged to be controversial. However, we wish to point out that it is used here only as the theoretical basis for considering the WLF parameter c_1 to be independent of pressure, a result that is supported by experimental data.

Time–temperature superposition of dielectric and viscoelastic data at atmospheric pressure has generally been represented by the Williams–Landell–Ferry equation,[2] which, with T_g as the reference temperature, can be written as

$$\log a_T = \frac{-c_1(T - T_g)}{c_2 + T - T_g} \tag{1}$$

where

$$a_T = \tau(T)/\tau(T_g) \tag{2}$$

is the ratio of the relaxation time at temperature T to that at T_g. An infinite value of log a_T occurs when $T = T_g - c_2 = T_\infty$. It was proposed by Williams et al.[2] that

$$c_1 = 1/2.303f_g \tag{3}$$

and

$$c_2 = f_g/\alpha_f \tag{4}$$

where f_g is the fractional free volume at the glass transition and α_f is the relative free volume expansion.

We now consider the application of eq 1 to high-pressure data. Since the relaxation time τ can be written as $(2\pi\nu_m)^{-1}$, where ν_m is the frequency of maximum loss at temperature T, eq 2 may be rewritten as

$$\log a_T = -\log (\nu_m(T)/\nu_g) \tag{5}$$

where ν_g represents the (hypothetical) frequency of maximum loss at T_g. Substitution in eq 1 leads to

$$\log \nu_m(T) = \log \nu_g + c_1 - c_1c_2/(T - T_\infty) \tag{6}$$

Since $(T - T_\infty)^{-1}$ tends to zero at high temperatures

$$c_1 = \log (\nu_0/\nu_g) \tag{7}$$

where ν_0 is the peak loss frequency. Equation 6 becomes

$$\log \nu_m(T) = \log \nu_0 - c_1c_2/(T - T_\infty) \tag{8}$$

This equation is of the same general form as the empirical Vogel or Tammann–Hesse equation used some 6 decades ago to represent the temperature dependence of viscosity. In fact, it forms the direct basis for the WLF equation. The reverse derivation from the WLF equation is nevertheless useful because eq 8 is expressed in terms of the WLF parameters c_1 and c_2 rather than an arbitrary "constant" B.

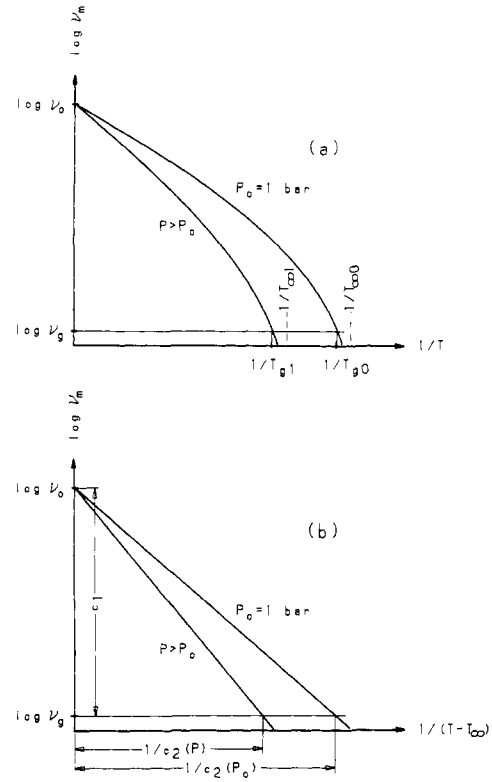

Figure 11. Schematic representation of the effect of pressure on (a) log ν_m vs. $1/T$ plots and (b) log ν_m vs. $1/(T - T_\infty)$ plots.

If it is assumed that the glass transition occurs at a constant fractional free volume, then it is apparent from eq 3 that c_1 will be independent of pressure.

It may be assumed that the frequency ν_g is the frequency characteristic of a typical scanning experiment, such as dilatometry or differential scanning calorimetry, and can be obtained at atmospheric pressure by the intersection of extrapolated dielectric data with the value of T_g obtained in a scanning experiment. This frequency, ν_g, can be taken as the *definition* of the glass transition and hence will be used to define the glass transition at pressures other than atmospheric. Since c_1 and ν_g are pressure-independent constants, it follows from eq 7 that ν_0 is also independent of pressure.

Equation 8 may thus be rewritten as

$$\log \nu_m(T,P) = \log \nu_0 - c_1c_2(P)/[T - T_\infty(P)] \tag{9}$$

This equation is identical in form with the following Vogel-type equation suggested by Williams:[12]

$$\log \nu_m(T,P) = \log \nu_0 - B(P)/[T - T_0(P)] \tag{10}$$

It is also similar in general shape to an empirical equation used by Williams,[9] particularly with regard to the invariance of ν_0 with pressure. This constant value of ν_0,[9] when combined with eq 7, provides experimental support for a constant value of c_1. Moreover, Miller[13] has shown that for poly(vinyl acetate) the Vogel term $B/(T_g - T_0)$ remains constant at 38.5 for pressures up to 0.8 kbar. Recognizing that $B \equiv 2.303c_1c_2$ and $T_0 \equiv T_\infty$, this means that $c_1 = 16.7$ independent of pressure.

From the foregoing, it is evident that a series of log ν_m vs. $1/T$ plots at different pressures are of the form shown schematically in Figure 11a; i.e. they all intersect at log ν_0. When eq 9 is used to plot the data, straight-line plots result that intersect at ν_0 but have differing slopes (Figure 11b). Experimental data may therefore be analyzed from

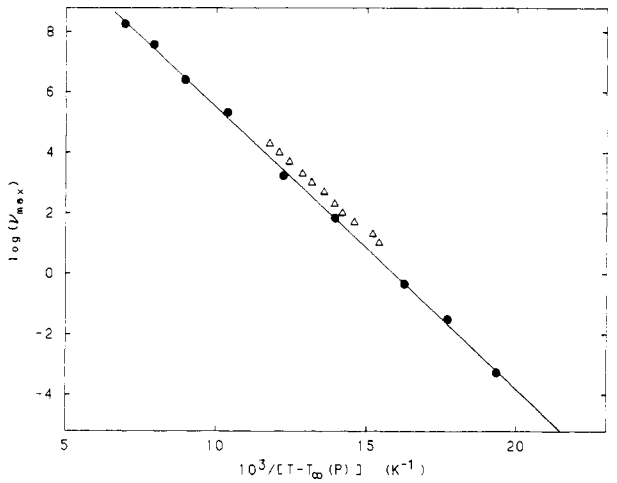

Figure 12. log ν_{max} vs. $1/(T - T_\infty)$ plot for the data of Bakule and Stoll[7] (●) and this work (△) at atmospheric pressure.

Table I
Values of c_1, c_2, c_1c_2, and T_∞ at Atmospheric Pressure

	Bakule and Stoll's data[7] [a]	this study	"universal"	Payne[15]
c_1	18.8	17.8	17.44	16.7
c_2 (K)	49.6	50.3	51.6	53.6
c_1c_2 (K)	933.3	897.6	899.9	895.1
T_∞ (K)	151.6	150.7		146.4

[a] Our analysis.

isobaric plots of log $\nu_m(T,P)$ vs. $(T - T_\infty(P))^{-1}$ and should be linear with a slope of $-c_1c_2$ and an intercept of log ν_0. The parameter $T_\infty(P)$ may be found by iterating to produce optimum linearity, as measured by the correlation coefficient of a linear least-squares fit. With c_1 constant, $c_2(P)$ is found from the slope of the optimized plot, and the glass transition temperature $T_g(P)$ may be calculated as $T_\infty(P) + c_2(P)$.

While linearization may be performed independently at each pressure studied, the large extrapolation (over about 10 times the experimental range) makes it very sensitive to even small errors in the experimental data. However, since ν_0 is independent of pressure, an accurate value of ν_0 may be obtained from appropriate atmospheric pressure data. The most extensive data available are those of Bakule and Stoll,[8] who were able to cover 12 decades of frequency. Their data have been fitted to eq 9, leading to maximum correlation for log $\nu_0 = 14.84$, $T_\infty = 151.6$ K, and $c_1c_2 = 933$ K (Figure 12).

Intersection of the extrapolated Bakule and Stoll data with the known glass transition temperature[14] for *cis*-polyisoprene of −72 °C leads to the value of log $\nu_g = -3.98$ whereas our data give log $\nu_g = -2.94$. Similar differences are obtained for values of c_1 and c_2. The values of c_1 are calculated from ν_0 and ν_g using eq 7 and are 17.8 for our data and 18.8 for Bakule and Stoll's data. Using c_1c_2/c_1 to calculate c_2 leads to 50.3 K for our data at atmospheric pressure and 49.6 for Bakule and Stoll's data. The values for all these parameters are compared to other estimates in Table I.

Analysis of the data presented in Figures 2–8 leads to the values of T_∞, c_2, and T_g shown in Table II. These values were used to compute the curves shown in Figure 10. The glass transition temperatures obtained as a function of pressure are presented in Figure 13. Also shown are the recent data of Sasuga and Takehisa,[3] who used a form of high-pressure dilatometry to determine glass transition temperatures under isothermal and isobaric conditions. Fitting of a second-order polynomial to our data leads to the equation

$$T_g(P) = -72.0 + 17.78P - 0.673P^2 \quad (11)$$

where T_g is in °C and P is in kbar. The correlation coefficient was 99.97%, and the use of higher orders leads to negligible improvement. Equation 11 was used for the extrapolated curve of Figure 13. In spite of the large extrapolation, a reasonable correspondence with the literature data[3] was found. The dotted line in Figure 13 represents a fit of our data together with the isobaric data of Sasuga and Takehisa.[3] The second-order polynomial (correlation coefficient 99.97%) resulting gives

$$T_g(P) = -72.0 + 16.42P - 0.23P^2 \quad (12)$$

The WLF energy term U^* for the process is given by

$$U^* = 2.303Rc_1c_2 \quad (13)$$

When computed with the values of c_1c_2 obtained from the slope of the log ν vs. $(T - T_\infty)^{-1}$ plots, U^* is found to increase with pressure from ~17 kJ/mol at atmospheric pressure to ~22 kJ/mol at 4 kbar.

Table II
Values of T_g, T_∞, c_1c_2, c_2, and U^* as a Function of Pressure

pressure, kbar	T_g, °C	T_∞, °C	c_1c_2, K	c_2, K	U^*, kJ/mol
0.001	−72.2	−122.5	897.6	50.3	17.2
0.34	−66.4	−120.2	956.0	53.8	18.3
0.69	−59.6	−115.2	989.2	55.6	18.9
1.72	−42.7	−99.8	1015.5	57.1	19.4
2.41	−33.6	−91.8	1033.9	58.2	19.8
3.45	−19.9	−86.2	1178.1	66.3	22.6

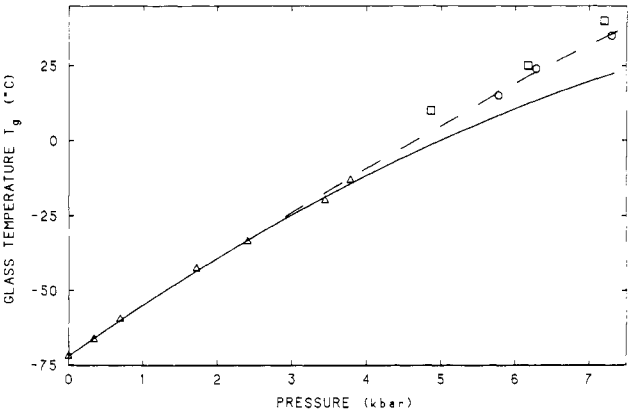

Figure 13. Glass transition temperature, T_g, as a function of pressure, in comparison with the isobaric (○) and isothermal (□) data of ref 3. The curves represent eq 11 (full) and 12 (dashed).

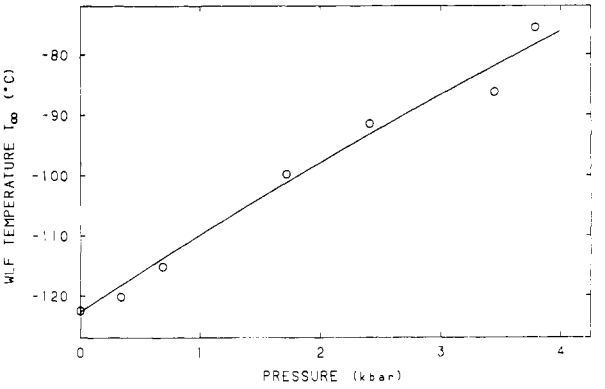

Figure 14. WLF temperature T_∞ as a function of pressure.

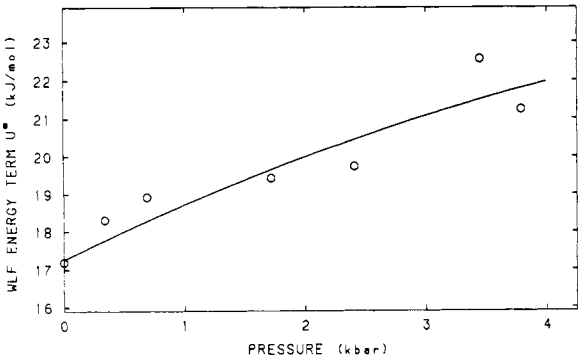

Figure 15. WLF energy term U^* as a function of pressure.

Table III
Atmospheric Pressure Values of T and dT/dP Corresponding to Dielectric Loss Maxima at Various Frequencies

description	log ν (ν in Hz)	$T_{P=0}$, °C	$(dT/dP)_{P=0}$, °C/kbar
10-kHz peak	4.00	−39.7	21.3
1-kHz peak	3.00	−46.6	20.0
100-Hz peak	2.00	−52.0	18.9
10-Hz peak	1.00	−57.6	18.9
T_g[a]	−2.94	−72.0	17.8
T_∞[a]	−∞	−122.5	13.2

[a] Extrapolated valu

The WLF terms T_∞ and U^* are plotted against pressure in Figures 14 and 15, respectively. The curves in these figures correspond to the fitted second-order polynomials

$$T_\infty(P) = -122.7 + 13.19P - 0.391P^2 \quad (14)$$

$$U^*(P) = 17.26 + 1.57P - 0.099P^2 \quad (15)$$

where T_∞ is in °C, U^* is in kJ/mol, and P is in kbar. The correlation coefficients are 99.5% and 96.7%, respectively, the latter reflecting the scatter of the U^* plot.

The rate of change of T_g with pressure was obtained by differentiating eq 11:

$$dT_g/dP = 17.78 - 0.673P \quad (16)$$

This value is at the low end of a list of empirical values tabulated by O'Reilly.[16]

Temperatures T_{max} corresponding to the dielectric loss peaks at various frequencies were also fitted to second-order polynomials against pressure. The low-pressure limit of dT_{max}/dP at various frequencies, obtained by differentiating these polynomials, are presented in Table III along with the extrapolated T_g and T_∞ values. Contrary to a common assumption (e.g., ref 16), dT_{max}/dP depends on frequency, even within the experimentally accessible frequency range. Williams[9] has reported a very similar frequency dependence of dT_{max}/dP for poly(methyl acrylate). Consequently, dT_{max}/dP at experimental frequencies (typically 1 kHz) cannot be considered equivalent to dT_g/dP.

The frequency dependence of dT_{max}/dP follows naturally from eq 9, which may be differentiated to give

$$\left(\frac{dT_{max}}{dP}\right)_\nu = \left(\frac{1}{2.303R}\right)\left(\frac{dU^*}{dP}\right)\left(\frac{1}{\log(\nu_0/\nu)}\right) + \frac{dT_\infty}{dP} \quad (17)$$

where U^* has been substituted from eq 13. Examination of eq 14 and 15 reveals that, at atmospheric pressure, eq 17 predicts that a plot of $(dT_{max}/dP)_\nu$ vs. $[\log(\nu_0/\nu)]^{-1}$ would be linear with a slope of 82.0 °C/kbar and an intercept of 13.2 °C/kbar. Atmospheric pressure dT_{max}/dP

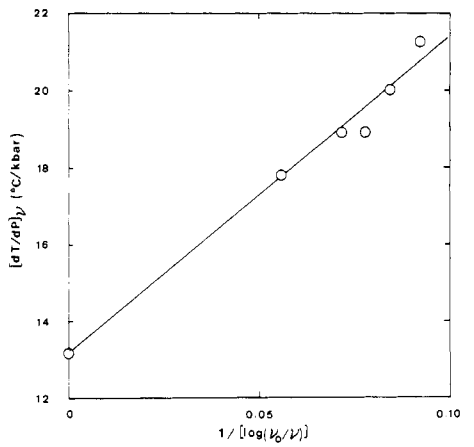

Figure 16. Plot of $(dT/dP)_\nu$ vs. $1/\log(\nu_0/\nu)$ at atmospheric pressure. The straight line is that predicted by eq 16.

Table IV
Comparison of Experimental and Predicted Values of dT/dP for *cis*-Polyisoprene at Atmospheric Pressure

	exptl	$\Delta\beta/\Delta\alpha$	$T_g V\Delta\alpha/\Delta C_p$
ref	this work	1	15
dT_g/dP, °C/kbar	17.8	21.2	20
dT_∞/dP	13.2		15

data from Table III are plotted in Figure 16 together with the predicted line, indicating internal consistency in our analyses.

McKinney et al.[1] have studied the effect of pressure on the dynamic compressibility of *cis*-polyisoprene vulcanized with 12% sulfur. Although the material used by McKinney is not identical with the unvulcanized material used in this study, the values obtained are nevertheless in fair agreement. McKinney et al. found that over the pressure range studied (0–1 kbar) their data could be satisfactorily reduced by a WLF analysis with the "universal" values of the constants. In this study, similarly, WLF constants very close to the "universal" values were obtained (see Table I).

McKinney et al. found that the temperature of the loss compliance maximum shifted with pressure at a rate of 24 °C/kbar. The equivalent value for our dielectric loss maxima was 20 °C/kbar at 1 kHz (see Table III).

Thermodynamic theories of the glass transition propose a second-order transition at a temperature T_2 (equivalent to T_∞ of the WLF formulation). The variation of a second-order transition temperature with pressure is given by the Ehrenfest relations.

Goldstein[17] has pointed out that both of these relations are valid only if a single ordering parameter is sufficient to characterize the excess thermodynamic properties of the liquid over those of the glass. According to Goldstein, if more than one ordering parameter is required, then

$$dT_g/dP = \Delta\beta/\Delta\alpha \quad (18)$$

if the excess volume determines T_g (as in free volume theories), while

$$dT_g/dP = T_g V\Delta\alpha/\Delta C_p \quad (19)$$

if either excess entropy or excess enthalpy determines T_g. Here, $\Delta\beta$, $\Delta\alpha$, and ΔC_p are the differences in compressibility, thermal expansion, and specific heat, respectively, between the glass and the liquid at the transition.

O'Reilly[16] has interpreted the data of McKinney et al.[1] to imply $\Delta\beta/\Delta\alpha = 24$ °C/kbar. However, McKinney et al. have $\Delta\beta = 1.02 \times 10^{-2}$ kbar (ΔB in their Table I) at

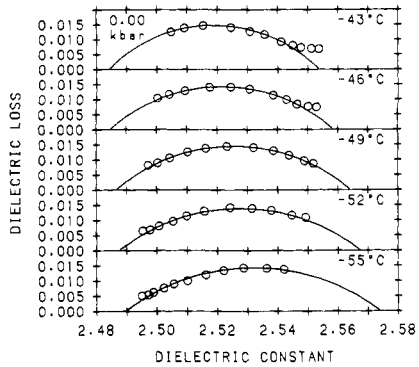

Figure 17. Cole–Cole plots at atmospheric pressure.

atmospheric pressure, and they have said that the "universal" value of $\alpha_f \simeq \Delta\alpha$ satisfactorily reduced their temperature–frequency data. Consequently, we have $\Delta\beta/\Delta\alpha = 1.02 \times 10^{-2}/4.8 \times 10^{-4} = 21.2$ °C/kbar. O'Reilly[16] has calculated the right-hand side of eq 19 to be 20 °C/kbar. These various values are compared in Table IV.

It is seen that the experimental value of dT_g/dP is closer to $T_gV\Delta\alpha/\Delta C_p$ (eq 19) than to $\Delta\beta/\Delta\alpha$ (eq 18). However, in view of the fact that the two predicted values differ by only about 1 °C/kbar, and because the $\Delta\beta/\Delta\alpha$ data[1] were obtained for a vulcanized sample, the data in Table IV cannot adequately differentiate between the validity of the free volume theories and the thermodynamic theories. The thermodynamic theories propose the second-order transition at T_2, not at T_g. Consequently, eq 19 might be expected to be better satisfied if $T_\infty \simeq T_2$ is used instead of T_g. Table IV shows that this correspondence is only fractionally better.

In this connection, it is perhaps appropriate to point out that some authors (e.g., ref 17 and 18) have interpreted experimental dT_g/dP data as support for excess-entropy or excess-enthalpy control of T_g, as opposed to excess-volume control of T_g. On the other hand, Havlicek et al.[19] have numerically calculated the molecular parameters of the Gibbs–DiMarzio model of glass formation for several polymers and conclude that the quantity most nearly constant at the glass transition is in fact the free volume. Their calculations also suggest that zero configurational entropy at T_2 and the free volume concept of the glass transition can be simultaneously valid.

Relaxation Time Distribution. Two shape parameters are frequently adequate to describe the distribution of relaxation times found in polymers (e.g., see ref 20). These are the Cole–Cole parameter, α, which is a measure of the width of the distribution and the Cole–Davidson parameter, β, which describes its asymmetry. [α and β in this section should not be confused with the thermodynamic quantities for which they were used earlier.] Both these parameters lie within the range ($0 < \alpha,\beta \leq 1$), the upper limit $\alpha = \beta = 1$ corresponding to the case of a single relaxation time (SRT) model. While these parameters were originally used independently, they have been combined[21] in the Havriliak–Negami equation.

Examination of the dielectric data presented in Figures 2–8 indicated that the distribution was fairly symmetric and could be adequately described in terms of a Cole–Cole analysis (i.e., $\beta = 1$). Values of the dielectric loss and constant were obtained at various temperatures and pressures by interpolating the isobaric–isochronal dielectric constant and loss data with a smoothed cubic-splines program and evaluating the resultant curves at several isothermal sections. Cole–Cole plots were generated from these data; a representative plot at atmospheric pressure is presented in Figure 17. The high-pressure Cole–Cole plots may be found in ref 5.

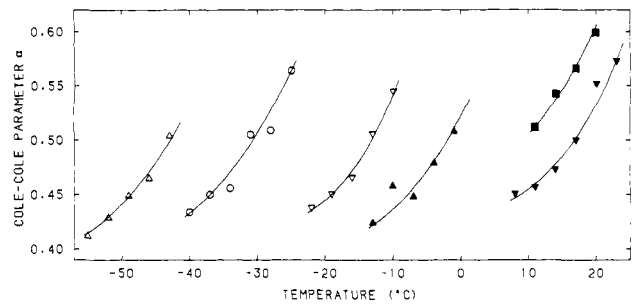

Figure 18. Cole–Cole parameter α as a function of temperature and pressure. Symbols as in Figure 10.

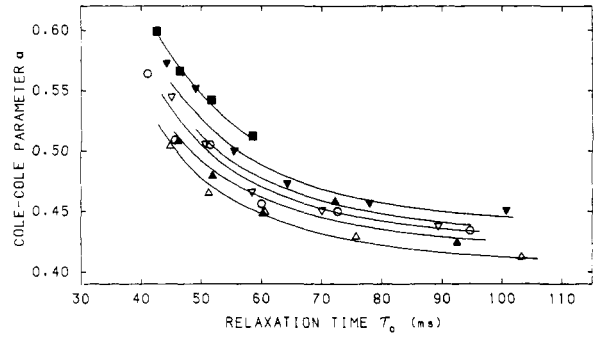

Figure 19. Cole–Cole parameter α as a function of relaxation time τ_0. Symbols as in Figure 10.

The useful temperature range of this analysis was limited by the experimental frequency scale (typically 3.3 decades). This temperature range was further limited on the high-temperature side by residual dc conductivity. Over the temperatures chosen, scatter in the data points gave rise to an uncertainty in the value of the Cole–Cole parameter, α, of about ±5%. The uncertainty in the relaxation strength $\Delta\epsilon = \epsilon_0 - \epsilon_\infty$ was comparable, but that in the actual limiting values ϵ_0 and ϵ_∞ was much higher. This is most likely due to random variations in the level of ionic impurity conduction in isopentane used as the hydraulic fluid, as well as small but variable alignment errors with the removable inner electrode.

The Cole–Cole parameter, α, thus obtained is plotted against temperature, at the various pressures, in Figure 18. Increasing temperature results in an increase in α, i.e., in a narrowing of the distribution. The α vs. T curves are shifted to higher temperatures at high pressures but remain fairly parallel.

Yoshihara and Work[22] have obtained precision dielectric data for poly(4-chlorostyrene) near the glass transition. There are significant differences between their data and ours. They have suggested that the shape parameter α is a function of the relaxation time τ_0 alone, irrespective of how τ_0 is varied (i.e., by changing temperature, solvent dilution, etc.). The relaxation time at a given temperature can be varied by the application of pressure as well, so their suggestion was evaluated by plotting, in Figure 19, α against log τ_0. The relaxation time τ_0 at a given temperature and pressure was obtained from the fitted WLF-type relations (eq 9 and Figure 10) and the conversion

$$\tau_0 = \omega^{-1} = (2\pi\nu)^{-1} \tag{20}$$

appropriate for a symmetric ($\beta = 1$) distribution.

It is apparent from Figure 19 that the data do not superpose. While the separation between the curves is not large, a clear trend is seen; α increases with pressure at a given relaxation time.

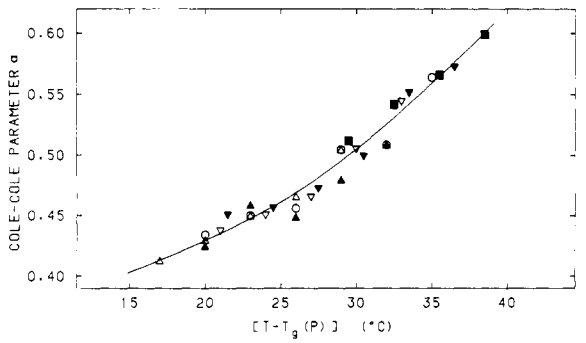

Figure 20. Cole–Cole parameters α as a function of shifted temperature, $T^* = T - T_g(P)$. Symbols as in Figure 10.

An alternative procedure would be to plot α against some shifted temperature. We have chosen a shifted temperature T^* to be defined as

$$R^* = T - T_g(P) \tag{21}$$

This definition merely causes a shift along the temperature axis such that the glass transition temperatures at all pressures would coincide. The resulting plot of α vs. T^* is presented in Figure 20 and shows good superposition. This would tend to indicate that α is determined primarily by proximity to the glass transition temperature (i.e., by $T - T_g$) for this particular polymer.

Yoshihara and Work's[22] values of the shape parameters ($\beta \simeq 0.5$, $\alpha \simeq 0.8$–0.9) for poly(4-chlorostyrene) are very different from those of this study ($\beta \simeq 1$, $\alpha \simeq 0.4$–0.6). While the uncertainty in our parameters is much higher than theirs, there is no question that their shape parameters are not compatible with our data. Examination of the values of these parameters for several amorphous polymers[20] indicates that many of them (PMMA, PMA, etc.) have higher α values for main-chain relaxation but lower values ($\alpha \simeq 0.3$–0.6) for side-group relaxation. However, *cis*-polyisoprene is devoid of large pendant side groups.

Boyd[23] has proposed that chain interactions due to small amounts of crystallinity and/or cross-linking in an "amorphous" polymer can alter the relaxation time distribution from asymmetric and narrow to symmetric and broad. One common polymer that has such a distribution is PVC.[24] While the rate of crystallization of *cis*-polyisoprene is essentially zero at room temperature, it is noticeable (though still quite slow) at lower temperatures, with a maximum at about −26 °C. It also has a gel component. Consequently, both crystallinity and cross-linking may be present in the dielectric sample. Also, as is well-known, the high molecular weight of *cis*-polyisoprene results in rubber elastic effects comparable to those of lightly cross-linked polymers. No attempt has been made to correlate the shape parameters with these properties, but over the time scales involved (cooling at ~1 °C/min) virtually no crystallinity could be detected by polarized light microscopy and would not be expected on the basis of the known kinetics of crystallization.[25]

A broadening of the relaxation time distribution in *cis*-polyisoprene with both crystallinity and cross-linking is apparent from published data. Bakule and Stoll[8] found that a sample that had been slowly cooled from the melt had a slightly larger relaxation strength, $\Delta\epsilon$, and a significantly smaller dielectric loss maximum, ϵ_m'', for the glass relaxation process at −40 °C than a sample that had been quenched. These changes were reversible. They have said nothing about the crystallinity of their samples, but it is reasonable to assume that the slow-cooled sample was more crystalline than the quenched one.

It is possible to calculate the Cole–Cole parameter, α, from their reported values of ϵ_m'' and $\Delta\epsilon$ using the geometric relation

$$\alpha = \frac{2}{\pi} \sin^{-1}\left(\frac{\epsilon_m''\Delta\epsilon}{(\epsilon_m'')^2 + (\Delta\epsilon/2)^2}\right) \tag{22}$$

A symmetric distribution was assumed, which is compatible with the shape of their loss curves. The resulting values are α(slow cooled) = 0.35 and α(quenched) = 0.46. The latter value is slightly smaller than that calculated in this work. The expected reduction in α with crystallinity is seen to be true.

The broadening of dielectric loss curves with cross-link density has been well established by Bakule and Havranek.[26] They found that over their experimental range, the empirical relation

$$\Delta_{0.7} = 0.311 \log V + 2.26 \tag{23}$$

related $\Delta_{0.7}$ (the width of the dielectric loss curve at $\epsilon'' = 0.7\epsilon_m''$) to the cross-link density V for the range $V = 10^{-5}$–10^{-3} mol/cm^3. Equation 23 applied for several different cross-linking systems. They explained this effect, in similar terms to Mason,[27] as the widening of the free volume distribution with increasing cross-link density. Adachi et al.[28] have found a similar broadening of dielectric loss curves for an acrylonitrile–butadiene random copolymer. It therefore seems likely that the value of α in *cis*-polyisoprene is a direct consequence of its high molecular weight and/or the gel content.

Acknowledgment. We thank Professors Richard H. Boyd and Graham Williams for many helpful comments. We also acknowledge the support of the Polymers Section at the National Science Foundation through the award of Grants DMR77-2108, 78-24696, and 81-06033.

References and Notes

(1) McKinney, J. E.; Belcher, H. V.; Marvin, R. S. *Trans. Soc. Rheol.* **1960**, *4*, 347.
(2) Williams, M. L.; Landel, R. F.; Ferry, J. D. *J. Am. Chem. Soc.* **1955**, *77*, 3701.
(3) Sasuga, T.; Takehisa, M. *J. Macromol. Sci., Phys.* **1977**, *B13*, 215.
(4) Norman, R. H. *Proc. Inst. Electr. Eng., Part 2A* **1953**, *100*, 41.
(5) Dalal, E. N. Ph.D. Dissertation, University of Utah, 1983.
(6) Sayre, J. A.; Swanson, S. R.; Boyd, R. H. *J. Polym. Sci., Polym. Phys. Ed.* **1978**, *16*, 1739.
(7) Sayre, J. A.; Boyd, R. H., unpublished data.
(8) Bakule, R.; Stoll, B. *Colloid Polym. Sci.* **1977**, *255*, 1176.
(9) Williams, G. *Trans. Faraday Soc.* **1964**, *60*, 1548, 1556; **1966**, *62*, 2091.
(10) Williams, G.; Watts, D. C. *NMR Basic Princ. Prog.* **1970**, *4*, 271.
(11) Williams, G.; Watts, D. C. *Trans. Faraday Soc.* **1971**, *67*, 2793.
(12) Williams, G., private communication.
(13) Miller, A. A. *Polymer* **1978**, *19*, 899.
(14) Wood, L. A. *Rubber Chem. Technol.* **1976**, *49*, 189.
(15) Payne, A. R. In "Rheology of Elastomers"; Mason, P., Wookey, N., Eds.; Pergamon Press: London, 1958.
(16) O'Reilly, J. M. *J. Polym. Sci.* **1962**, *57*, 429.
(17) Goldstein, M. *J. Chem. Phys.* **1963**, *39*, 3369.
(18) Sasabe, H.; Saito, S. *Polym. J.* **1972**, *3*, 631.
(19) Havlicek, I.; Vojta, V.; Ilavsky, M.; Hrouz, J. *Macromolecules* **1980**, *13*, 357.
(20) McCrum, N. G.; Read, B. E.; Williams, G. "Anelastic and Dielectric Effects in Polymeric Solids"; Wiley: New York, 1967.
(21) Havriliak, S.; Negami, S. *Polymer* **1967**, *8*, 161.
(22) Yoshihara, M.; Work, R. N. *J. Chem. Phys.* **1980**, *72*, 5909.
(23) Boyd, R. H., private communication.
(24) Ishida, Y. *Kolloid Z.* **1960**, *168*, 29.
(25) Phillips, P. J.; Edwards, B. C. *J. Polym. Sci., Polym. Phys. Ed.* **1975**, *13*, 1819.
(26) Bakule, R.; Havranek, A. *J. Polym. Sci., Polym. Symp.* **1975**, *No. 53*, 347.
(27) Mason, P. *Polymer* **1964**, *5*, 625.
(28) Adachi, H.; Adachi, K.; Kotaka, T. *Polym. J.* **1980**, *12*, 329.